GEOPHYSICAL RESEARCH LETTERS, VOL. 33, L24706, doi:10.1029/2006GL027468, 2006



# Solar and anthropogenic forcing of tropical hydrology

Drew T. Shindell,[1] Greg Faluvegi,[1] Ron L. Miller,[1] Gavin A. Schmidt,[1] James E. Hansen,[1] and Shan Sun[1]

Received 18 July 2006; revised 21 September 2006; accepted 17 November 2006; published 27 December 2006.

[1] Holocene climate proxies suggest substantial correlations between tropical meteorology and solar variations, but these have thus far not been explained. Using a coupled ocean-atmosphere-composition model forced by sustained multi-decadal irradiance increases, we show that greater tropical temperatures alter the hydrologic cycle, enhancing the climatological precipitation maxima in the tropics while drying the subtropical subsidence regions. The shift is enhanced by tropopause region ozone increases, and the model captures the pattern inferred from paleoclimate records. The physical process we describe likely affected past civilizations, including the Maya, Moche, and Ancestral Puebloans who experienced drought coincident with increased irradiance during the late medieval (~900–1250). Similarly, decreased irradiance may have affected cultures via a weakened monsoon during the Little Ice Age (~1400–1750). Projections of 21st-century climate change yield hydrologic cycle changes via similar processes, suggesting a strong likelihood of increased subtropical drought as climate warms. **Citation:** Shindell, D. T., G. Faluvegi, R. L. Miller, G. A. Schmidt, J. E. Hansen, and S. Sun (2006), Solar and anthropogenic forcing of tropical hydrology, *Geophys. Res. Lett.*, *33*, L24706, doi:10.1029/2006GL027468.

## 1. Introduction

[2] Changes in the hydrologic cycle, including droughts and flooding, are among the most immediate and important projected consequences of global warming for human society. While shifts in the hydrologic cycle are a robust feature of model simulations of global warming, it is difficult to evaluate model realism using observations of the recent past. In response to increasing greenhouse gas concentrations, climate models simulate more water vapor in the atmosphere and exhibit reduced vertical overturning in the tropics, with ensuing increases in equatorial precipitation and decreases in the subtropics [*Held and Soden*, 2006]. Analyses of observations, however, provide ambiguous evidence for recent trends in vertical circulation and the underlying tropical lapse rate [*Chen et al.*, 2002; *Mitas and Clement*, 2005, 2006; *Santer et al.*, 2005]. Precipitation changes are also uncertain due to the large inherent variability, the high degree of spatial inhomogeneity and the short duration of modern measurements. Paleoclimate records cover many centuries, however, and proxies from multiple sources suggest that hydrological changes are correlated at multi-decadal to century timescales with solar variations, especially for the intensity of the Indian Monsoon [*Fleitmann et al.*, 2003; *Wang et al.*, 2005a] and for drought occurrence in the subtropics of the Americas [*Cook et al.*, 2004; *deMenocal*, 2001; *Haug et al.*, 2003; *Hodell et al.*, 2001; *Rein et al.*, 2004]. As the response of the hydrologic cycle to projected greenhouse gas increases is similar to these historical changes, paleoclimate studies may provide valuable insight into the mechanisms underlying modern climate change.

[3] Models have not been able to produce statistically significant responses similar to the relationships inferred from proxies, however, and the processes behind them have remained unclear. This is perhaps not surprising since irradiance variations seem to have been small, and are largest at wavelengths that do not reach the Earth's surface or even the lower atmosphere. Variations are particularly large in the UV, and these wavelengths are absorbed in the stratosphere, where they also increase the ozone concentration via oxygen photolysis [*Haigh*, 1996; *Shindell et al.*, 1999], augmenting stratospheric heating. Limited computational resources have restricted prior simulations of historical climate to either emphasize the lower atmosphere and ocean at the expense of the upper atmosphere, or to include the upper atmosphere but with simplified ocean and/or chemical models. Our own previous simulations, for example, included a mixed-layer ocean with fixed circulation and parameterized stratospheric chemistry, which did not allow for ozone transport or for composition changes below the tropopause [*Shindell et al.*, 2001].

## 2. Experimental Setup

[4] Here we present simulations of the climate response to solar variations using the NASA Goddard Institute for Space Studies (GISS) modelE atmospheric GCM [*Schmidt et al.*, 2006] coupled to a fully dynamic ocean. The model includes fully interactive atmospheric chemistry extending from the surface to the lower mesosphere [*Shindell et al.*, 2006]. The configuration used here was a horizontal resolution of 4 by 5 degrees (latitude by longitude) with 23 vertical layers in the atmosphere, and including a gravity-wave drag (GWD) parameterization in the stratosphere. The HYCOM dynamic ocean model includes 16 vertical layers with horizontal resolution of 2 by 2 cos (latitude) degrees, and produces a reasonable magnitude of El Niño-Southern Oscillation (ENSO)-like variability.

[5] Sunspots and cosmogenic proxy data provide information about historical variations in solar output, but calibration is difficult. Estimates based on sun-like stars had reported that during the most pronounced long-term recent low, the Maunder Minimum (~1645–1715), the sun's output was reduced by several times the amplitude of an ~11-year solar cycle [*Lean*, 2000]. Newer evidence,

[1]NASA Goddard Institute for Space Studies and Earth Institute at Columbia University, New York, New York, USA.


0094-8276/06/2006GL027468$05.00

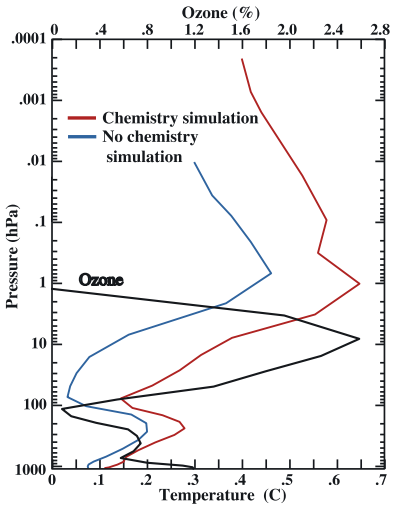


**Figure 1.** Tropical (32 N–32 S) average temperature (C) difference between increased and decreased irradiance in simulations with and without coupled chemistry (blue and red, bottom scale). The response without chemistry has been scaled by 2/3 to match the forcing used in the coupled chemistry simulations (0.19 W/m$^2$ at the tropopause). The ozone response (%) to irradiance changes in the coupled chemistry run is also shown (black, top scale).

however, indicates that observations do not provide appropriate stellar analogues, leading to suggestions that extended minima are simply akin to persistent solar cycle minima with no longer-term background change and thus an amplitude of one-half the ~11-year solar cycle [*Foukal et al.*, 2004]. We impose a full solar cycle perturbation (~0.19 W/m$^2$ instantaneous radiative forcing at the tropopause, equivalent to 1.1 W/m$^2$ change in solar output) as a mid-range estimate. This is in good agreement with recent model-based estimates [*Wang et al.*, 2005b]. Given the uncertainty in this forcing, we concentrate our comparison with observations on the spatial pattern of the response rather than its precise magnitude. The imposed irradiance changes included spectral variations based on modern observations, which show greatly enhanced variability at shorter wavelengths relative to the visible over a solar cycle. Atmospheric concentrations of long-lived species and emissions of short-lived species were set to preindustrial values. Simulations with +1/2 and −1/2 the solar cycle irradiance change were started using initial conditions derived from a control run (without chemistry) of several centuries. The model equilibrated (climate drift <0.001 C/yr) with the solar perturbations and coupled chemistry in ~30 years. All results are presented as differences between the +1/2 and −1/2 solar cycle runs over 70 years of subsequent integration, providing an appropriate simulation of the multi-decadal climate response to an extended period of altered irradiance.

[6] Ideally, the role of the many individual potential factors influencing the climate response to solar forcing could be studied with multiple sensitivity studies using the identical model. This is precluded by the impractically long integration time (~9 months). It is nevertheless insightful to compare these results with prior simulations of the response to spectrally-resolved solar forcing performed with a 20-layer version of modelE run without including interactive chemistry, without a GWD parameterization, and coupled to a different ocean [*Hansen et al.*, 2005b]. As discussed in the supplementary material[1], we believe that the role of differences in GWD and the ocean are secondary, and that the comparison emphasizes the effects of chemistry. Those runs used a tropopause forcing of 0.29 W/m$^2$ based on the older reconstruction [*Lean*, 2000], so we scale the results by 0.66 to match our forcing.

## 3. Results

[7] The combined influence of ozone and irradiance increases enhances stratospheric heating (Figure 1). The Brewer-Dobson circulation also decreases slightly (~2% in the coupled composition runs), contributing to heating of the tropical lower stratosphere [*Kodera and Kuroda*, 2002; *Matthes et al.*, 2006]. Comparing the vertical profiles of temperature response (Figure 1) shows clearly that stratospheric heating is much larger in the new runs, and that the enhancement is greatest at levels where ozone increases (and above, where there is greater absorption by greenhouse gases of outgoing longwave radiation from the warmer lower levels). In contrast, the magnitudes and spatial patterns of the tropical and subtropical surface temperature responses over the oceans, and the spatial structure of the zonal mean temperature response, are broadly similar in the two sets of simulations (see supplemental material). This suggests that the differences between the two models' tropical responses are likely attributable primarily to the ozone chemical response rather than the oceans or the GWD. Further experiments are required to verify this.

[8] The greater warming in the coupled chemistry simulations extends down to the tropical upper troposphere, where it more than triples the net response. Increased ozone near the tropopause results primarily from the enhanced photochemistry driven by the increased irradiance, with an additional influence from reduced upward transport of ozone-destroying radicals such as nitrogen oxides. The ozone increases exert a small positive radiative forcing (~0.03 W/m$^2$) and the added upper tropospheric heating reduces the tropical lapse rate.

[9] Models simulating global warming exhibit a consistent response of the hydrological cycle [*Held and Soden*, 2006]. As the surface warms, boundary layer moisture increases rapidly following the exponential Clausius-Clapeyron law. For a constant circulation, convergence of the horizontal moisture flux follows this same scaling. Convergence is balanced by evaporation minus precipitation (E-P), so that in wet regions where P exceeds E, precipitation increases. Conversely, in dry regions, where evaporation dominates, precipitation is reduced, because the moisture export exceeds the increase in evaporation.

[10] The model's response to solar forcing is consistent with these theoretical principles. In response to surface warming (Figure 2), precipitation increases along the equator while the subtropics generally show drying (Figure 3, bottom). The zonal mean anomalies show substantially larger subtropical drying in the coupled composition model,

[1] Auxiliary materials are available in the HTML. doi:10.1029/2006GL027468.

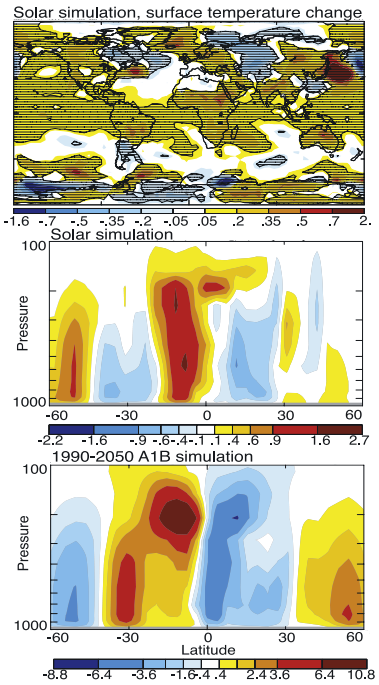


**Figure 2.** (top) Annual average surface air temperature (C) difference between increased and decreased irradiance averaged over 70 years in the simulation with coupled chemistry. Hatching indicates 95% statistical significance, global mean increase is 0.10. (middle) The zonal mean streamfunction ($10^9$ kg/s) difference from the coupled ocean-atmosphere-composition solar simulation, and (bottom) the trend in a transient simulation over 1990–2050 using observed forcings through 2003 and A1B projections thereafter. A positive streamfunction is defined as showing clockwise overturning circulation. Thus the negative anomalies stretching roughly from the equator to 20–30 N and the positive anomalies in the Southern tropics indicate reduced upwelling along the equator and reduced subsidence in the subtropics.

where they are highly statistically significant (99%) while they are only marginally so in the earlier runs despite comparable surface warming (Figure 3, bottom). This contrasting response suggests a contribution by circulation changes to the anomalous moisture flux, in addition to the effect of warming and moistening at the surface. This conclusion is supported by the results of another composition-climate model [*Matthes et al.*, 2006]. That study held SSTs fixed, but found similar patterns of precipitation and circulation response to solar forcing, however only in January. This suggests that the tropical tropospheric overturning is influenced by stratosphere-troposphere coupling, which is strongest in NH winter, in addition to the effects of surface warming.

[11] Over the Americas, the most pronounced terrestrial precipitation anomalies are reductions over Mexico and the Southwestern US (Figure 3). Numerous tree-ring, fire and lake salinity records from these areas indicate reduced precipitation and a pronounced increase in drought frequency during periods of increased irradiance over the past 1200 years [*Cook et al.*, 2004]. Isotopes in lake sediments from the Yucatan suggest a similar solar-precipitation relationship [*Hodell et al.*, 2001], as do those in ocean sediments reflective of precipitation over central Peru [*Rein et al.*, 2004] and Patagonia [*Stine*, 1994] for the past two to three millenia. Conversely, an ocean sediment record reflective of precipitation in northern tropical South America (strongly reflective of precipitation in the inter-tropical convergence zone (ITCZ)) indicates wetter conditions with increased irradiance [*Haug et al.*, 2003]. The climate model's pattern of increased precipitation near the equator (in the ITCZ in some areas, while directly along the equator in others) and decreases at subtropical to middle latitudes of

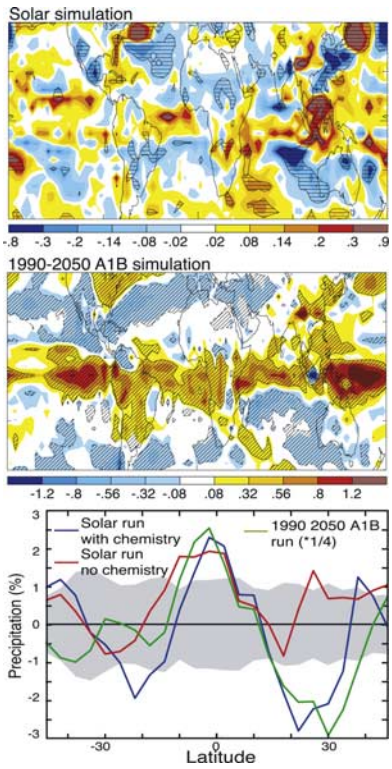


**Figure 3.** (top) Annual average precipitation (mm/day) difference between increased and decreased irradiance averaged over 70 years in the simulation with coupled chemistry. Hatching indicates 90% statistical significance. (middle) The trend in the transient simulation over 1990–2050. With the larger response in the A1B run, virtually all colored areas are statistically significant at the 90% level. (bottom) Zonal mean precipitation changes from the indicated runs are shown (in percent), with the solar run without chemistry scaled by 2/3 to the same forcing as the coupled chemistry run, the transient response scaled by 1/4 (to highlight pattern similarity), and shading indicating the 95% significance level in the coupled chemistry run. Percent changes are larger in some regions than in the zonal mean (e.g. the SW US decreases are 5–10% in the solar simulation, and 10–20% in the unscaled transient). The global mean surface temperature responses in the model are 0.10 C in the solar/chemistry run, 0.08 C in the earlier solar run without chemistry, and 1.25 C in the A1B transient. Thus the precipitation response per degree of surface warming in the solar/chemistry runs is roughly three times larger than in the A1B simulations.

both hemispheres is thus broadly consistent with the paleoclimate results.

[12] In the Indian monsoon region, maritime precipitation changes are again fairly zonally uniform, but terrestrial precipitation shows eastward shifts leading to increases in areas where the monsoon brings heavy rain (Figure 3, top). The largest effects are increases over Bangladesh, China, parts of SE Asia and Indonesia accompanied by decreases to the west over parts of India (though the model's climatology places too much monsoon precipitation over eastern South Asia relative to the central and western portions). Anomalies in the monsoon region arise almost exclusively during NH summer (when they have roughly double the magnitude of the annual average response), while equatorial and ITCZ anomalies are present in summer and winter. The results indicate an intensification of regional monsoonal precipitation as irradiance increases, in accord with suggestions from paleoclimate records in stalagmites and ocean sediments [*Fleitmann et al.*, 2003; *Wang et al.*, 2005a] and with modern data [*Kodera*, 2004; *van Loon et al.*, 2004]. Reductions in monsoon rainfall may have contributed to cultural events in Asia such as the collapse of Angkor early in the Little Ice Age.

[13] Many of the paleoclimate records have been interpreted as indicating shifts in the ITCZ position with solar variations. This does not vary in the climate model, though it may be that the model's 4 degree latitude resolution is insufficient to resolve such motions. Simulated shifts do occur for other forcings such as orbital changes or Younger Dryas-type events. Some records have been interpreted as indicating that solar changes modulate ENSO variability [*Cook et al.*, 2004; *Rein et al.*, 2004]. In the simulations, the tropical Pacific warms everywhere (Figure 2, top), however, with no change in the E-W gradient. Thus the simulations produce the observed precipitation patterns without coupled ocean feedbacks creating more La Niña-like ocean conditions. Solar forcing does induce increased precipitation in the tropical western Pacific, however (Figure 3, top). The resulting additional latent heating there sets up La Nina-like conditions in the atmosphere, which have been linked to drought in the SW US [*Meehl and Hu*, 2006; *Schubert et al.*, 2004]. These regional circulation changes can then enhance the precipitation decreases associated with the zonal mean subtropical drying processes discussed previously. Prolonged La Nina-like conditions in response to increased irradiance has been seen in a simplified ENSO model [*Mann et al.*, 2005]. Such additional La Nina modulation of ocean circulation, which would lead to similar rainfall increases in the Western Pacific and decreases in the SW US, could amplify the response seen here.

[14] The NH extratropics show increased zonal winds at mid-latitudes, projecting onto an annular pattern as in our previous experiments [*Shindell et al.*, 2001]. The current simulations, with a much more sophisticated model, show a less zonally symmetric response, however, with shifts of both the Aleutian and Azores pressure systems. The model produces enhanced warming over Europe, maximizing in the NE, and over the NE US and central Canada but cooling over the Labrador Sea area and at least part of N Africa (see Figure S1), consistent with proxy reconstructions as in the work by *Shindell et al.* [2001]. Further discussion of the extratropical responses will be presented elsewhere.

## 4. Relation to Global Warming Projections

[15] We also performed transient climate simulations using the same setup as the solar runs without chemistry. These experiments ran from 1880 to 2003 using observed forcings [*Hansen et al.*, 2005a], then using future projections. We analyze 1990–2050 trends from an IPCC A1B scenario simulation, an illustrative example with a global mean annual average surface temperature increase of 1.25 C during this period (the range in our model was 0.94 C (B1) to 1.28 C (A2)). Modeled climate sensitivity to solar and GHG forcings seems to be quite similar. The value is 0.52 C/W/m$^2$ in the solar/chemistry equilibrium run and 0.38 C/W/m$^2$ in the A1B run for which a smaller value is expected owing to the transient setup and lack of positive ozone feedback.

[16] Comparison of the zonal mean tropical circulation response with that seen in the solar simulations reveals that both display reduced vertical overturning (Figure 2), a response consistent with theory [*Held and Soden*, 2006]. The reduction in equatorial upwelling is clear in both simulations. While both also show reduced downwelling in the subtropics/mid-latitudes, details in the extratropics are rather different. Not surprisingly, the broadly similar patterns of surface warming and altered circulation lead to overall precipitation trends in the GHG run that in many respects echo those seen in the solar experiments (Figure 3) and in other models [*Held and Soden*, 2006]. Interestingly, though the zonal mean precipitation changes show a similar pattern, the response per degree surface warming is roughly three times larger in the solar/chemistry simulation than in the A1B run. Some of this enhancement may be due to stratosphere-troposphere coupling, or to the changes in tropospheric ozone, which affect regional patterns of heating (Figure S2) and can thus alter circulation. However, in the equatorial band where precipitation increases, the solar run without chemistry also shows much greater precipitation sensitivity (response per degree surface warming) than the A1B run. The greater equatorial sensitivity to solar forcing may arise from differences in the forcings themselves. GHG forcing is spatially uniform, while solar forcing preferentially affects the surface in clear-sky areas, especially in the subtropics, influencing the circulation response [*Meehl et al.*, 2003]. Thus theoretical models of the zonal mean response to surface warming can account for much of the simulated zonal mean precipitation change, but certainly do not describe the entire response.

[17] In fact, though the patterns of zonal mean precipitation responses are qualitatively similar in the solar and GHG cases, there are important spatial differences. These are especially apparent in the equatorial Pacific. The GHGs induce a large precipitation increase centered on the equator throughout the Pacific (Figure 3, middle). In contrast, the response to solar forcing shows equatorial enhancements in the Western Pacific, but enhancements along the ITCZ bands in the Eastern Pacific, with a relative minimum along the equator (Figure 3, top). Precipitation increases over the Indian Ocean show a similar dichotomy between equatorial response in the GHG runs and ITCZ enhancement in the

solar case. The Pacific response to solar forcing is consistent with observations during NH winter [*van Loon et al.*, 2006] and previous modeling that showed enhancement of regional precipitation in response to increased solar irradiance [*Meehl et al.*, 2003]. Both solar and GHG forcing lead to drying of the subtropics, however, especially over SW North America (Figure 3).

[18] The results suggest that a warmer climate will lead to enhancement of the climatological precipitation maxima in the equatorial Western Pacific, the ITCZ and in the Asian monsoon, and decreased precipitation over the American Southwest and Mexico. These changes take place largely via processes for which we have a fundamental physical understanding [*Held and Soden*, 2006]. Indeed, a weakening of the vertical Walker circulation in the Pacific has recently been reported [*Vecchi et al.*, 2006] that operates on similar principles but is primarily in the zonal direction while we focus on meridional anomalies within the zonally-averaged circulation. Our results demonstrate that the same processes may have driven analogous variations in the tropical hydrologic cycle in the past. Thus we believe it is justified to have a fairly high degree of confidence in projections of future warming and their associated large-scale changes in precipitation.

[19] Historical variations in tropical hydrology have been linked to dramatic cultural changes and even collapses. Drought in the Americas, for example, may have contributed to the Classic Maya collapse, shifts in the habitation patterns of the Moche in what is now Peru, and to city abandonment by the Ancestral Puebloans in the American Southwest [*deMenocal*, 2001; *Haug et al.*, 2003; *Hodell et al.*, 2001]. While modern societies are in many ways much better equipped to deal with drought, they have vastly greater populations living in semi-arid regions, increasing drought vulnerability. Furthermore, the 1990–2050 climate forcing (3.28 W/m$^2$) is more than 15 times our mid-range historical solar forcing estimate, implying that future changes are likely to greatly exceed those in the past despite a reduced precipitation sensitivity for GHGs relative to solar forcing (as in Figure 3). Precipitation decreases, combined with greater evaporation in a warmer climate, could lead to very severe drought conditions. The projected changes thus have a potential to cause substantial harm, especially in water-stressed regions such as the American Southwest, Mexico, parts of North Africa and the Near East, and Australia.

[20] **Acknowledgments.** Thanks to R. Ruedy, P. deMenocal, G. Meehl, I. Held, and NASA's Atmospheric Chemistry Modeling and Analysis Program.

## References

Chen, J., B. E. Carlson, and A. D. Del Genio (2002), Evidence for strengthening of the tropical general circulation in the 1990s, *Science*, *295*, 838–841.

Cook, E. R., C. A. Woodhouse, C. M. Eakin, D. M. Meko, and D. W. Stahle (2004), Long-term aridity changes in the western United States, *Science*, *306*, 1015–1018.

deMenocal, P. B. (2001), Cultural responses to climate change during the late Holocene, *Science*, *292*, 667–673.

Fleitmann, D., S. J. Burns, M. Mudelsee, U. Neff, J. Kramers, A. Mangini, and A. Matter (2003), Holocene forcing of the Indian monsoon recorded in a stalagmite from southern Oman, *Science*, *300*, 1737–1739.

Foukal, P., G. North, and T. Wigley (2004), A stellar view on solar variations and climate, *Science*, *306*, 68–69.

Haigh, J. D. (1996), The impact of solar variability on climate, *Science*, *272*, 981–984.

Hansen, J., et al. (2005a), Earth's energy imbalance: Confirmation and implications, *Science*, *308*, 1431–1435.

Hansen, J., et al. (2005b), Efficacy of climate forcings, *J. Geophys. Res.*, *110*, D18104, doi:10.1029/2005JD005776.

Haug, G. H., D. Gunther, L. C. Peterson, D. M. Sigman, K. A. Hughen, and B. Aeschlimann (2003), Climate and the collapse of Maya civilization, *Science*, *299*, 1731–1735.

Held, I. M., and B. J. Soden (2006), Robust responses of the hydrological cycle to global warming, *J. Clim.*, *19*, 5686–5699.

Hodell, D. A., M. Brenner, J. H. Curtis, and T. Guilderson (2001), Solar forcing of drought frequency in the Maya lowlands, *Science*, *292*, 1367–1370.

Kodera, K. (2004), Solar influence on the Indian Ocean monsoon through dynamical processes, *Geophys. Res. Lett.*, *31*, L24209, doi:10.1029/2004GL020928.

Kodera, K., and Y. Kuroda (2002), Dynamical response to the solar cycle, *J. Geophys. Res.*, *107*(D24), 4749, doi:10.1029/2002JD002224.

Lean, J. (2000), Evolution of the Sun's spectral irradiance since the Maunder Minimum, *Geophys. Res. Lett.*, *27*, 2425–2428.

Mann, M. E., M. A. Cane, S. E. Zebiak, and A. Clement (2005), Volcanic and solar forcing of the tropical Pacific over the past 1000 years, *J. Clim.*, *18*, 447–456.

Matthes, K., Y. Kuroda, K. Kodera, and U. Langematz (2006), Transfer of the solar signal from the stratosphere to the troposphere: Northern winter, *J. Geophys. Res.*, *111*, D06108, doi:10.1029/2005JD006283.

Meehl, G. A., and A. Hu (2006), Megadroughts in the Indian monsoon region and southwest North America and a mechanism for associated multo-decadal Pacific sea surface temperature anomalies, *J. Clim.*, *19*, 1605–1623.

Meehl, G. A., W. M. Washington, T. M. L. Wigley, J. M. Arblaster, and A. Dai (2003), Solar and greenhouse gas forcing and climate response in the twentieth century, *J. Clim.*, *16*, 426–444.

Mitas, C. M., and A. Clement (2005), Has the Hadley cell been strengthening in recent decades?, *Geophys. Res. Lett.*, *32*, L03809, doi:10.1029/2004GL021765.

Mitas, C. M., and A. Clement (2006), Recent behavior of the Hadley cell and tropical thermodynamics in climate models and reanalyses, *Geophys. Res. Lett.*, *33*, L01810, doi:10.1029/2005GL024406.

Rein, B., A. Lückge, and F. Sirocko (2004), A major Holocene ENSO anomaly during the medieval period, *Geophys. Res. Lett.*, *31*, L17211, doi:10.1029/2004GL020161.

Santer, B. D., et al. (2005), Amplification of surface temperature trends and variability in the tropical atmosphere, *Science*, *309*, 1551–1556.

Schmidt, G. A., et al. (2006), Present day atmospheric simulations using GISS ModelE: Comparison to in-situ, satellite and reanalysis data, *J. Clim.*, *19*, 153–192.

Schubert, S. D., M. J. Suarez, P. J. Pegion, R. D. Koster, and J. T. Bacmeister (2004), On the cause of the 1930s Dust Bowl, *Science*, *303*, 1855–1859.

Shindell, D. T., D. Rind, N. K. Balachandran, J. Lean, and P. Lonergan (1999), Solar cycle variability, ozone, and climate, *Science*, *284*, 305–308.

Shindell, D. T., G. A. Schmidt, M. E. Mann, D. Rind, and A. Waple (2001), Solar forcing of regional climate change during the Maunder Minimum, *Science*, *294*, 2149–2152.

Shindell, D. T., G. Faluvegi, N. Unger, E. Aguilar, G. A. Schmidt, D. Koch, S. E. Bauer, and R. L. Miller (2006), Simulations of preindustrial, present-day, and 2100 conditions in the NASA GISS composition and climate model G-PUCCINI, *Atmos. Chem. Phys.*, *6*, 4427–4459.

Stine, S. (1994), Extreme and persistent drought in California and Patagonia during mediaeval time, *Nature*, *369*, 546–549.

van Loon, H., G. A. Meehl, and J. M. Arblaster (2004), A decadal solar effect in the tropics in July–August, *J. Atmos. Sol. Terr. Phys.*, *66*, 1767–1778.

van Loon, H., G. A. Meehl, and D. J. Shea (2006), Coupled air-sea response to solar forcing in the Pacific region during northern winter, *J. Geophys. Res.*, doi:10.1029/2006JD007378, in press.

Vecchi, G. A., B. J. Soden, A. T. Wittenberg, I. M. Held, A. Leetmaa, and M. J. Harrison (2006), Weakening of tropical Pacific atmospheric circulation due to anthropogenic forcing, *Nature*, *441*, 73–76.

Wang, Y., et al. (2005a), The Holocene Asian monsoon: Links to solar changes and North Atlantic climate, *Science*, *308*, 854–857.

Wang, Y.-M., J. Lean, and N. R. Sheeley (2005b), Modeling the Sun's magnetic field and irradiance since 1713, *Astrophys. J.*, *625*, 522–538.

G. Faluvegi, J. E. Hansen, R. L. Miller, G. A. Schmidt, D. T. Shindell, and S. Sun, NASA Goddard Institute for Space Studies, 2880 Broadway, New York, NY 10025, USA. (dshindell@giss.nasa.gov)